minerals

MDPI

Communication

Reducing the Presence of Clusters in Bubble Size Measurements for Gas Dispersion Characterizations

Luis Vinnett [1,2,*], Benjamín Urriola [1], Francisca Orellana [1], Camila Guajardo [1] and Alex Esteban [1]

[1] Department of Chemical and Environmental Engineering, Universidad Técnica Federico Santa María, Valparaíso 2390123, Chile
[2] Automation and Supervision Centre for Mining Industry, CASIM, Universidad Técnica Federico Santa María, Valparaíso 2390123, Chile
* Correspondence: luis.vinnett@usm.cl

Abstract: This short communication evaluates a new strategy to sample bubbles in gas dispersion characterizations. Bubble size is measured in a bidimensional flotation cell using the McGill bubble size analyzer under different types of frothers, frother concentrations and superficial gas rates. The original design of this bubble viewer is modified, changing the deflecting system to photograph only a fraction of the bubbles entering the device. As a result, the new design increases the ability to successfully identify bubbles by a maximum of 20% using an automated algorithm. This increase is caused by a reduction in the formation of clusters in the visual field. The improvement, which is a function of the operating conditions, is most significant in the transition from ellipsoidal/ellipsoidal–turbulent regimes (no frother or low frother concentrations) to conditions with an over-agglomeration of bubbles in the visual field (high superficial gas rates and high frother concentrations). A comparison of the bubble size parameters obtained from the original and proposed deflecting systems shows that the new design does not distort the estimated bubble size distributions. To complement the research findings, alternative sampling designs, using new or existing segmentation algorithms, are then proposed to improve gas dispersion characterizations at different scales.

Keywords: gas dispersion; flotation; bubble size; clusters; sampling

Citation: Vinnett, L.; Urriola, B.; Orellana, F.; Guajardo, C.; Esteban, A. Reducing the Presence of Clusters in Bubble Size Measurements for Gas Dispersion Characterizations. *Minerals* **2022**, *12*, 1148. https://doi.org/10.3390/min12091148

Academic Editor: Kevin Galvin

Received: 25 August 2022
Accepted: 8 September 2022
Published: 10 September 2022

1. Introduction

Flotation performance depends on several operating conditions, with gas dispersion being a critical variable that influences the process efficiency and separation rate. The flotation rate constant has proven to be proportional to bubble surface area flux, collection efficiency and froth recovery [1–3]. Bubble size plays a role in affecting each of these parameters, which explains its impact on the process performance. Bubble size has been proposed as an operating variable to improve the recovery of fine and coarse particles, as recently discussed by Hassanzadeh et al. [4]. New flotation technologies have incorporated alternative mechanisms to disperse gas, focusing on higher collection efficiencies. Bubble size is typically characterized by the bubble size distribution (BSD) and Sauter mean diameter ($D_{32} = \Sigma d_i^3/\Sigma d_i^2$). The latter corresponds to an equivalent diameter with the same volume-to-surface ratio as the evaluated population [1,5–8].

Several devices have been proposed to estimate the bubble size in flotation [9–13]. Systems based on bubble viewers along with image processing tools have received more attention than others because of their trade-off between the number of sampled bubbles and their applicability at different scales. The bubble viewers are initially filled with conditioned water, which is displaced by the gas as the bubbles rise into the chamber. The sampling system was designed such that the bubbles are photographed in a bidimensional plane to avoid BSD distortions due to variable depths of field. On the plane, the photographed bubbles tend to collide, leading to an increase in the observation of clusters of bubbles, as illustrated by several authors at different scales [14–16].

Two approaches have been typically followed to deal with clusters of bubbles in BSD characterizations: (i) removal of objects with low shape factors, and (ii) object segmentation. The first strategy has been widely used in the flotation literature [17–19], even though significant biases have been observed in BSD estimations [20–22]. The Hough [20,23] and Watershed [10,24] transforms have been proposed for circle detection and object segmentation, respectively, to identify bubbles in clusters. Although these techniques reduce bubble removal, the results have not yet been satisfactory in industrial applications [14].

Changes in the sampling design to reduce the presence of clusters have been scarce. An evident modification to the bubble viewers is the use of narrow sampling tubes [25]. However, this approach has proven to change the observed gas dispersion patterns at high superficial gas rates and high frother concentrations [26]. Azgomi et al. [27] measured bubble size in a laboratory-scale flotation column. This column was designed with an expansion in the section where bubble size was measured. The results showed that the gas holdup decrease in the sampling point was effective in the reduction of the bubbles observed in the visual field. Yet, though this approach allowed for simpler bubble size estimations, it required changes to the flotation machines instead of the measurement system. More recently, an in situ bubble viewer was evaluated at laboratory scale [28]. The ParticleView^{TM} V19 probe containing a camera was used to directly measure bubble size in the collection zone. Bubbles were identified in a field of view of 1300 μm × 890 μm. This measurement system did not include any mechanism to photograph bubbles in a bidimensional plane. Thus, the presence of bubbles in clusters may have been lower with respect to conventional bubble viewers. However, the measurement system had variable depths of field and was limited to spherical regimes.

This short communication presents an alternative design for sampling bubbles in flotation. The McGill bubble size analyzer (MBSA) [29] was used for data acquisition. The deflecting system of this device was modified to divert only a fraction of the bubbles to the visual field, with the aim of reducing the presence of clusters. The effectiveness of this design was evaluated at laboratory scale under different operating conditions.

2. Materials and Methods

Bubble size measurements were conducted at the laboratory scale in the two-dimensional flotation cell schematized in Figure 1. This forced-air cell represents a slice of an industrial flotation cell (upper radial section), with a 140 cm × 140 cm cross-section and a width of 15 cm. The air flow rate was regulated at J_G = 0.4, 1.2 and 2.0 cm/s and fed from 24 porous spargers. These superficial gas rates were chosen according to the typical values reported by Vinnett, Yianatos and Alvarez [5] for industrial flotation machines. For each J_G value, three commercial frothers were assessed to expand the set of experimental conditions: AeroFroth® 70 (Cytec, Woodland Park, NJ, USA), OrePrep® F-507 (Cytec, Woodland Park, NJ, USA) and Flotanol® 9946 (Clariant Mining Solutions, Louisville, KY, USA). AeroFroth® 70 contains methyl isobutyl carbinol (MIBC) and diisobutyl ketone, with MIBC as the main component [30]; OrePrep® F-507 contains 30–60% glycol and other non-hazardous ingredients to 100% [30]; Flotanol® 9946 corresponds to a 2-ethyl hexanol distillation bottom [31]. The experimental critical coalescence concentrations (at J_G = 0.4 cm/s) were approximately 12.6 ppm, 7.1 ppm and 6.2 ppm for AeroFroth® 70, OrePrep® F-507 and Flotanol® 9946, respectively. Frother concentrations of 0, 2, 4, 8, 16 and 32 ppm were evaluated for each reagent and superficial gas rate. Thus, 18 experimental conditions were run per frother type.

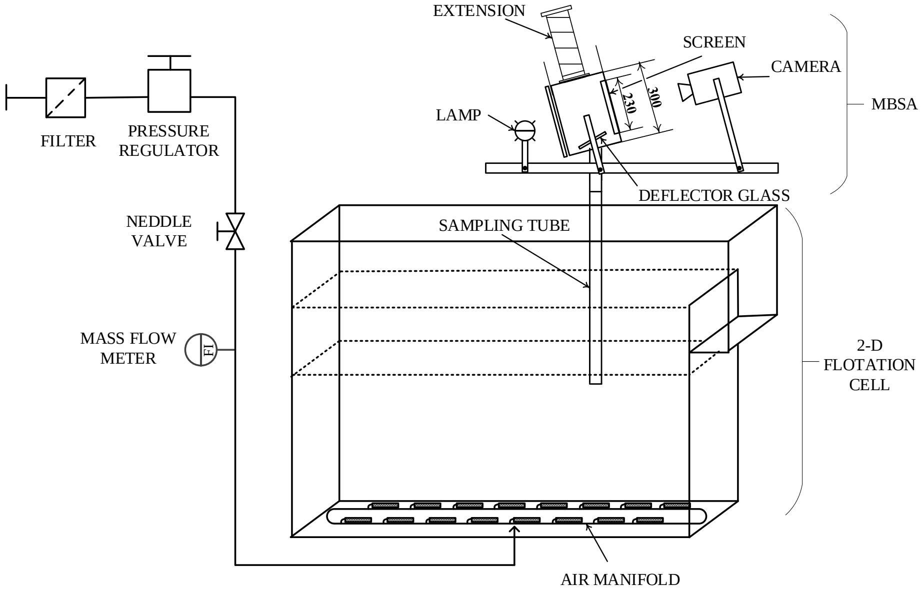

Figure 1. Two-dimensional flotation cell and installation of the McGill bubble size analyzer (modified from [32]).

The McGill bubble size analyzer (MBSA) [29] was used to sample and record the bubble images. The MBSA chamber was initially filled with conditioned water at the same frother concentration as the 2D cell. The water was displaced by the sampled bubbles, and the air was accumulated at the top of the chamber. The original design included a deflector glass that diverts the rising bubbles to measure the BSD in a single two-dimensional plane. A digital video camera (Teledyne Dalsa, Waterloo, ON, Canada) was used for image acquisition at a sampling rate of one frame per second and a resolution of 0.056 mm/pxl. All measurements were conducted for 3 min.

Two types of deflectors were used to evaluate the potential to reduce the presence of clusters in the visual field. Figure 2 presents the original deflector of 7.7 cm × 10 cm (Figure 2a) and an alternative design (Figure 2b). In the former, all sampled bubbles were diverted to the visual field for image acquisition. The alternative design involved a sampling tube extension inside the MBSA chamber (1 in Figure 2b) and a shorter deflector glass of 4 cm × 10 cm (2 in Figure 2b) to divert approximately 50% of the bubbles to the visual field. Bubbles that were not diverted to the MBSA screen were accumulated in the glass arrangement in Figure 2b consisting of plates 3 (3.5 cm × 15 cm) and 4 (5 cm × 15 cm), and directed far from the visual field. This design guaranteed that only a fraction of the sampled bubbles was recorded for image processing. It should be noted that the alternative deflecting system did not change the characteristics of the bubbles entering the sampling tube. For each experimental condition, the BSD measurements were alternately conducted using the original and new deflectors.

A semi-automated tool from the Image Processing Toolbox of MATLAB (The MathWorks Inc., Natick, MA, USA) was implemented to characterize the bubble size populations. The recorded images were analyzed from their black and white representations. The algorithm sequentially applied bubble identification based on solidity [33] to detect regular bubbles (i.e., isolated spheres and ellipsoids). The size of these regular bubbles was then estimated as an equivalent ellipsoid diameter. Objects with low solidity were sequentially segmented using Watershed and Hough transforms [20,34]. The previous steps define the automatic algorithm (Figure 3b, 45 mm × 35 mm). Table 1 presents the relevant parameters and thresholds for each of these automated techniques. These parameters were defined to obtain a trade-off between the number of successfully identified bubbles and the presence of false positives (e.g., clusters of bubbles identified as single bubbles). The semi-automated tool was then complemented with manual processing. False positives were first removed from the analysis, as shown in Figure 3c. Complex clusters and irregular bubbles were then manually estimated, as illustrated in Figure 3d. Thus, no bubbles were removed from the image analysis. The results from the entire semi-automated algorithm were used as references for comparison purposes. For each experimental condition, 180 images were recorded. From this set of images, a subset was randomly chosen for analysis. A minimum of 1500 bubbles were processed per experimental condition. For the cases with no frother, all images were analyzed. A minimum of 10 images were processed for conditions with a high number of bubbles per frame (e.g., high J_G and high frother concentration). A field of view of 45 mm × 35 mm was chosen in all cases.

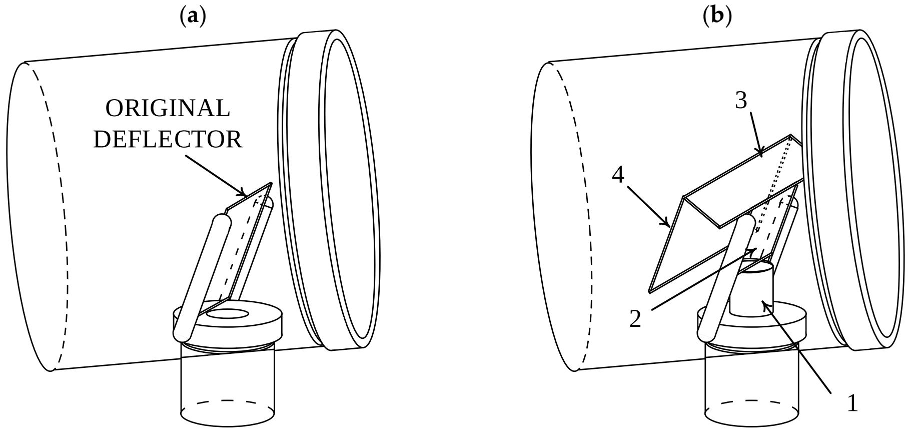

Figure 2. Diagrams of the MBSA deflectors: (**a**) original design; (**b**) new design.

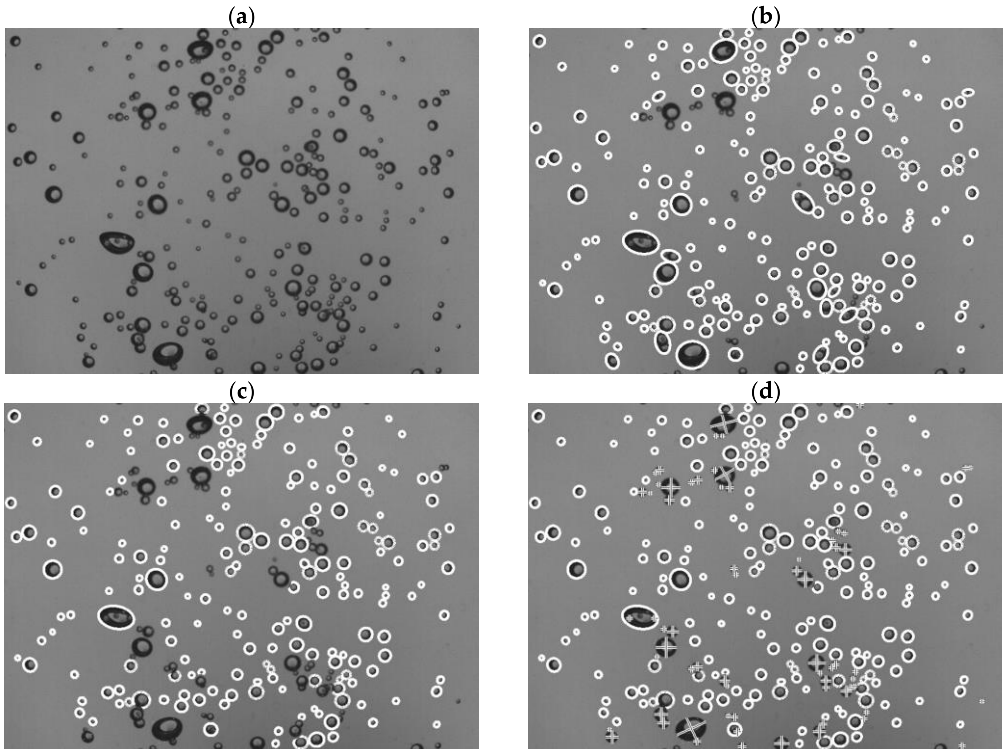

Figure 3. Example of a processed image (45 mm × 35 mm): (**a**) original image; (**b**) automatic image processing; (**c**) false-positive removal; (**d**) manual processing.

Table 1. Parameters of each image processing technique.

Technique	Threshold	Sensitivity	Edge Threshold
Solidity	0.93	-	-
Watershed + Solidity	0.93	-	-
Hough	-	0.80	0.66

3. Results

The efficacy of the new deflecting system to reduce the percentage of non-identified bubbles was evaluated. The algorithm described in Section 2 was used as the automated image processing tool. Figure 4 compares the percentage of bubbles that were manually characterized using the original and new deflectors, for each J_G value and type of frother. Figures 4a, 4b and 4c shows the comparisons for AeroFroth®70 and J_G = 0.4, 1.2 and 2.0 cm/s, respectively. Figures 4d, 4e and 4f, and Figures 4g, 4h and 4i present the same comparisons as a function of J_G for OrePrep®F-507 and Flotanol®9946, respectively. The results are shown as a function of the frother concentrations. The percentage of bubbles manually characterized included those that were not automatically identified and the false positives that were corrected in the analysis. Conditions under no frother were combined to increase bubble populations. A decrease in the non- and erroneously identified bubbles was typically observed when using the new deflector. The maximum increase in the successfully identified bubbles by the automated algorithm was approximately 20% for AeroFroth® 70 and J_G = 2.0 cm/s, which corresponded to a relative increase of about 38%. The improvement was strongly dependent on the operating conditions (i.e., type of frother, frother concentration and superficial gas rate). As the bubble size distributions transition from ellipsoidal (low J_G) or ellipsoidal–turbulent (high J_G) and spherical regimes when increasing the frother concentrations, the bubble shapes and bubble concentrations determine the capacity of the image processing techniques to identify bubbles. At 0 ppm and low frother concentrations the BSDs were governed by ellipsoidal and irregular bubbles whose shapes were not changed by the new deflector. Thus, the differences in the identified bubbles were not significant under those operating conditions. At a higher J_G (2.0 cm/s) and high frother concentrations, the significant agglomeration of bubbles in the visual field typically led to low or moderate–low improvements in bubble identification using the new deflector. Thus, the highest increase in the automatically identified bubbles was observed in the transition between conditions under ellipsoidal/ellipsoidal–turbulent regimes and those leading to over-agglomeration of bubbles in the visual field. This transition depended on the type of frother and superficial gas rates.

Figure 5 illustrates the percentages of bubbles observed in clusters at a 4 ppm frother concentration when using the original and new deflectors in the bubble sampling. The results are presented for the three types of frothers and superficial gas rates. The conditions at 4 ppm were chosen to allow for manual bubble counting with no significant bias. The percentage of clusters was also significant in all cases at this frother concentration. The new deflecting system decreased the number of bubbles observed in clusters. The magnitude of this improvement depended on the type of frother and the superficial gas rate. The absolute decreases were in the ranges of 1.6%–6.6%, 6.3%–11.1% and 6.1%–8.7%, for J_G = 0.4, 1.2 and 2.0 cm/s, respectively. These ranges represented relative improvements of 8%–17%, 15%–31% and 15%–20%, respectively. The results from Figure 5 show that the bubble sampling provided by the new deflecting system increased the number of automatically identified bubbles due to a reduction in their presence in clusters.

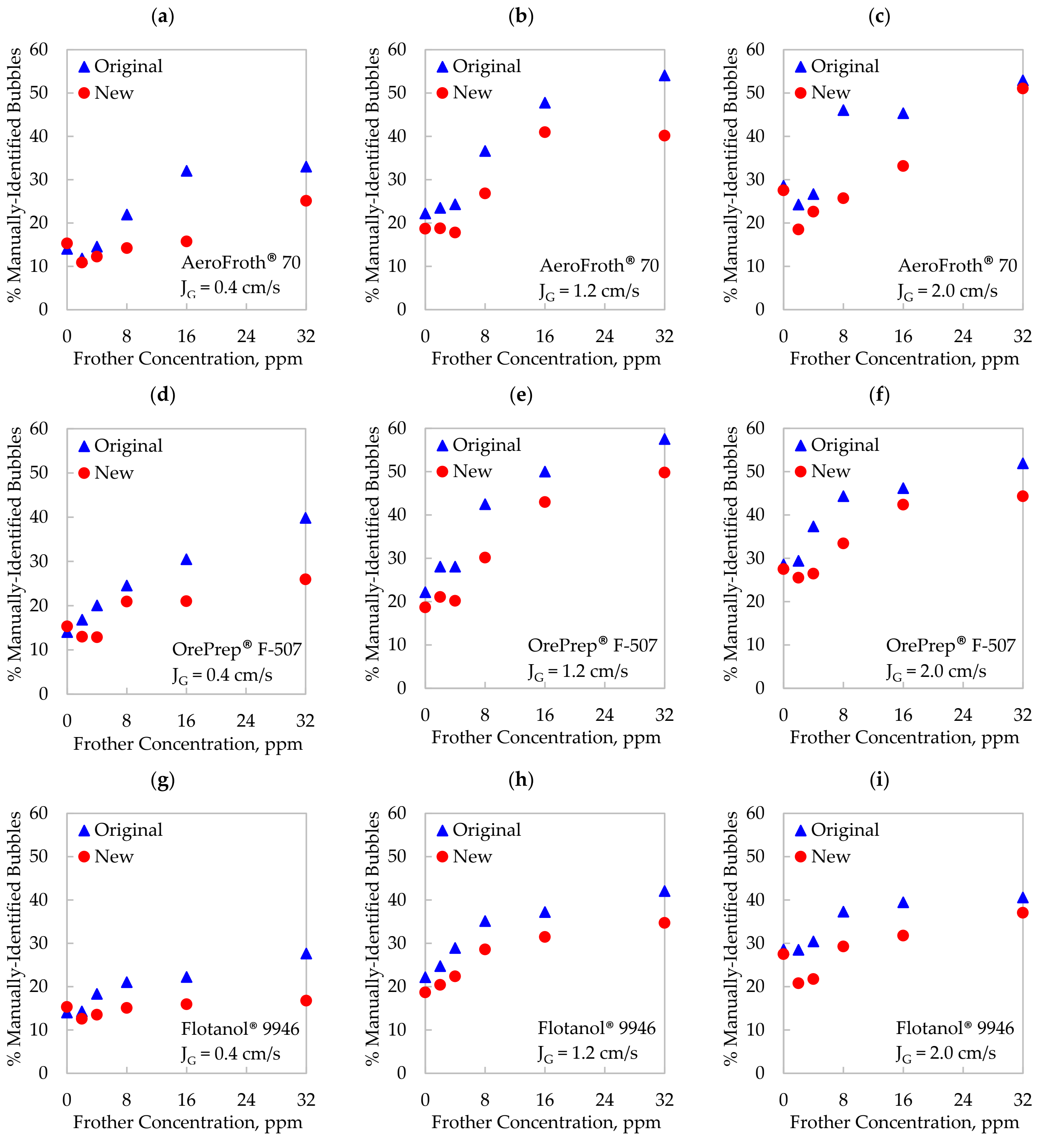

Figure 4. Comparison of the percentages of bubbles that were manually identified when using the original and the new deflectors. Operating conditions: AeroFroth® 70, (**a**) J_G = 0.4 cm/s, (**b**) J_G = 1.2 cm/s, (**c**) J_G = 2.0 cm/s; OrePrep® F-570, (**d**) J_G = 0.4 cm/s, (**e**) J_G = 1.2 cm/s, (**f**) J_G = 2.0 cm/s; Flotanol® 9946, (**g**) J_G = 0.4 cm/s, (**h**) J_G = 1.2 cm/s, (**i**) J_G = 2.0 cm/s.

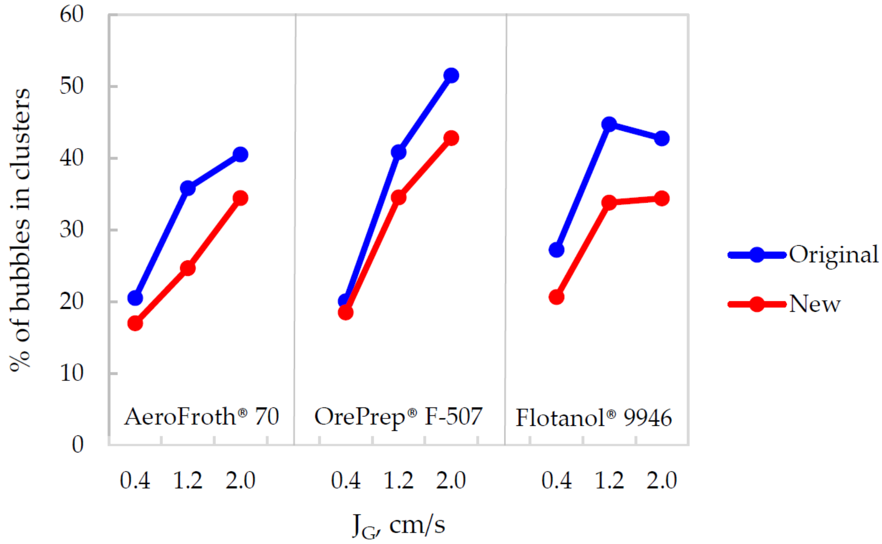

Figure 5. Percentage of bubbles in clusters under the original and new deflectors at a 4 ppm frother concentration.

Figure 6a,b compare the mean (D_{mean}) and Sauter mean diameters, respectively. These results were obtained from the original and new deflectors. In Figure 6a, the new sampling mechanism did not significantly change the location indexes of the BSDs, as also presented in Appendix A, for the bubble size median (D_{50} in Figure A1c). The Sauter mean diameter also presented a good agreement between the evaluated measurement systems, with moderately higher variability. As the Sauter mean diameter is more sensitive to extreme values, two experimental conditions presented higher deviations, which were caused by the presence of a low percentage of large bubbles (cap-shaped bubbles). However, this sensitivity was not biased toward one of the measurement systems. Appendix A presents the same comparison for percentiles 10 and 90 of the BSDs. From all these statistical indexes, the new deflecting system did not distort the bubble size distributions with respect to the original design.

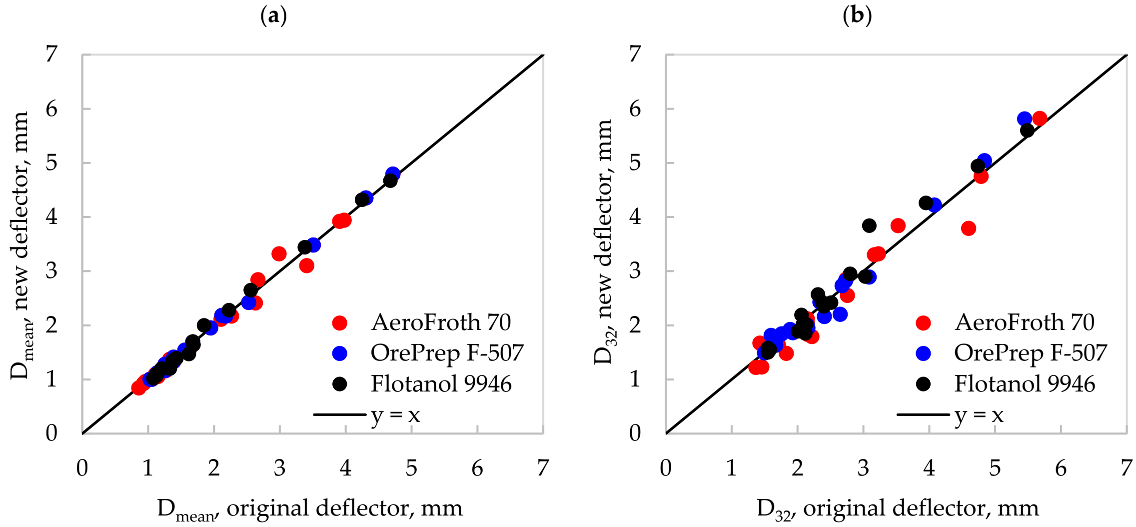

Figure 6. Comparison of the (**a**) mean bubble size and (**b**) Sauter mean diameter when using the original and new deflecting systems, as assessed using the McGill bubble size analyzer.

4. Discussion and Future Work

The identification of bubbles by only shape factors has proved to be biased [20–22], which has led to alternative algorithms for bubble size characterizations [10,20,23,24].

These algorithms have mainly been focused on the characterizations of bubbles in clusters by object segmentation and circle detection. However, these techniques have not led to satisfactory results in all flotation systems [14]. To date, scarce assessments of alternative sampling strategies have been reported in flotation literature. Results from Figures 4–6 and Figure A1 indicated that moderate changes in the bubble sampling allow for a reduction in the presence of bubbles in clusters, with no bias in the BSD estimations. Less bubbles in clusters make it possible for simpler image processing techniques or for a reduction in the computational costs for object segmentation. Although the new deflector led to satisfactory results at laboratory scale, more efforts must be made to reduce the formation of clusters in the visual field under high superficial gas rates and high frother concentrations. As the over-agglomeration of bubbles in the visual field has been common in industrial measurements leading to bias for $D_{32} > 2.0$ mm [14], further developments are being investigated to expand these results for gas dispersion characterizations at large scale. As shown here, bubble sampling has not been completely solved. Although the proposed strategy led to an improvement in the bubble size measurements, other possible drawbacks require specific studies for adequate gas dispersion characterizations. For example, stereological problems in bubble identification, population size for adequate bubble size estimations, and wall effect and solid presence at different scales, must be taken into consideration in future developments.

5. Conclusions

From laboratory flotation tests, the potential to reduce the number of bubbles photographed in clusters was evaluated as a strategy to improve gas dispersion characterizations. Using a modification for the McGill Bubble Size Analyzer, the following findings were obtained:

- A new deflecting system that allowed a fraction of the sampled bubbles to be photographed was effective in reducing clusters of bubbles in the visual field. This improvement strongly depended upon the experimental conditions (i.e., frother types and concentrations and superficial gas rates).
- The maximum improvement in the number of bubbles automatically identified was 20% (absolute), using the new deflector. This result corresponded to a relative increase of 38%.
- The new deflecting system led to better performances in the ability to automatically identify bubbles when transitioning from ellipsoidal/ellipsoidal-turbulent regimes (no frother or low frother concentrations) to conditions with an over-agglomeration of bubbles in the visual field (high superficial gas rates and high frother concentrations).
- The new sampling system allowed more bubbles to be automatically identified with no significant differences in the estimated statistical parameters of the bubble size distributions.

The study of new sampling strategies in bubble size measurements proved to have potential to improve gas dispersion characterizations. As automatic algorithms have not led to satisfactory results at large scale, it is estimated that less clusters in bubble size measurements may potentially improve BSD estimations in industrial flotation machines. The new deflecting design will be then assessed at large scale to detect opportunities for improvements in gas dispersion characterizations.

Author Contributions: Methodology, L.V. and B.U.; software, L.V.; formal analysis, L.V., B.U., F.O., C.G. and A.E.; writing—original draft preparation, L.V. and F.O.; writing—review and editing, L.V.; supervision, L.V.; project administration, L.V.; funding acquisition, L.V. All authors have read and agreed to the published version of the manuscript.

Funding: Funding for the process modeling and control research was provided by ANID, project Fondecyt 1201335, and Universidad Técnica Federico Santa María, project PI_LIR_2021_78.

Conflicts of Interest: The authors declare no conflict of interest.

Appendix A

Figure A1 shows comparisons of the 10th (Figure A1a), 90th (Figure A1b) and 50th percentiles (Figure A1c) of the estimated bubble size distributions when using the original and new deflecting systems in the MBSA. These three percentiles were consistent between the evaluated measurement schemes, which proved that the proposed deflecting system did not distort the estimated BSDs compared to the original MBSA design.

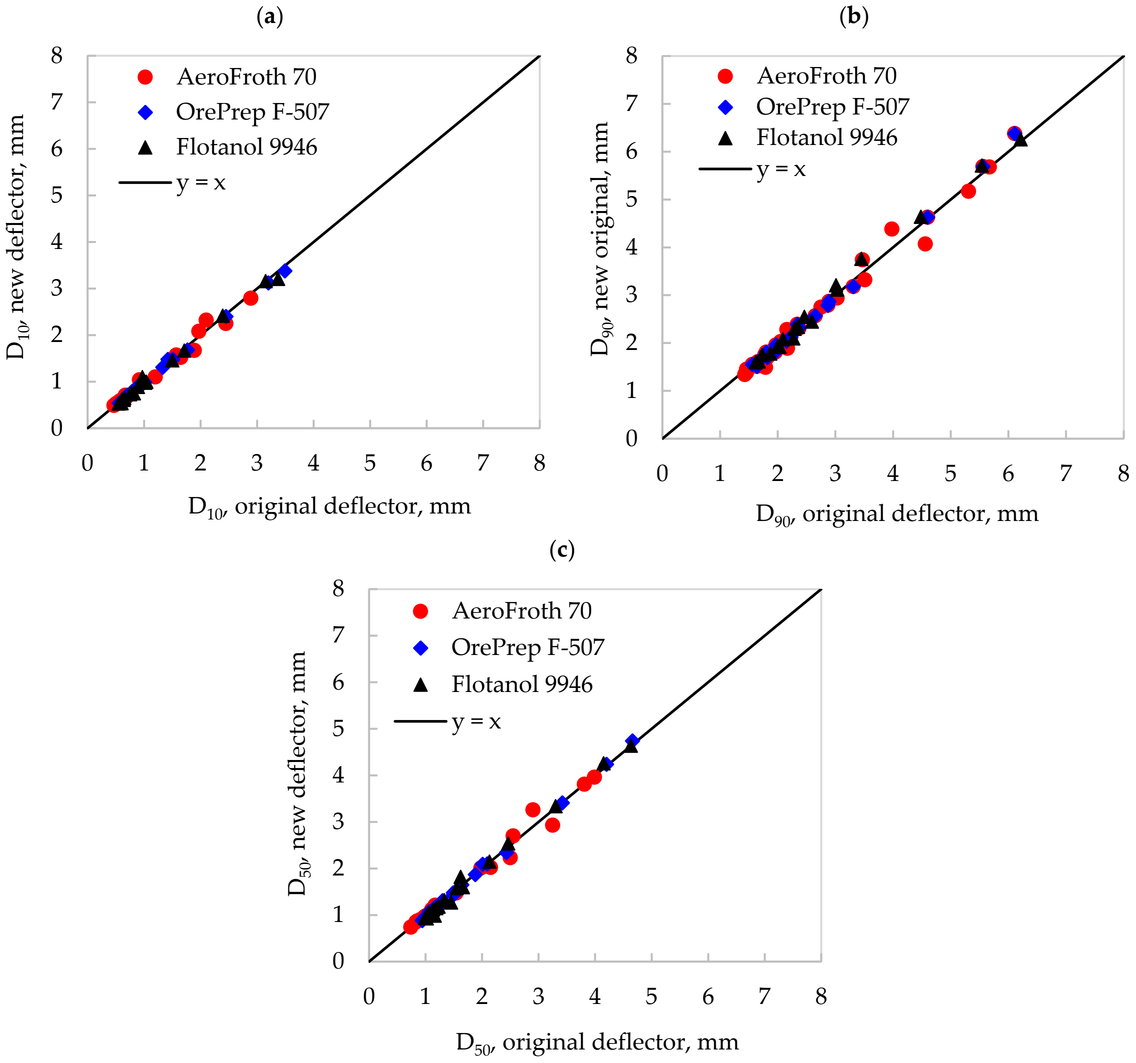

Figure A1. Comparison of different percentiles of the BSDs when using the original and new deflecting systems in the McGill bubble size analyzer: (**a**) 10th percentile (D_{10}), (**b**) 90th percentile (D_{90}) and (**c**) 50th percentile or median (D_{50}).

References

1. Gorain, B.; Franzidis, J.; Manlapig, E. Studies on impeller type, impeller speed and air flow rate in an industrial scale flotation cell. Part 4: Effect of bubble surface area flux on flotation performance. *Miner. Eng.* **1997**, *10*, 367–379. [CrossRef]
2. Gorain, B.; Napier-Munn, T.; Franzidis, J.-P.; Manlapig, E. Studies on impeller type, impeller speed and air flow rate in an industrial scale flotation cell. Part 5: Validation of k-Sb relationship and effect of froth depth. *Miner. Eng.* **1998**, *11*, 615–626. [CrossRef]
3. Finch, J.A.; Dobby, G.S. *Column Flotation*; Pergamon Press: Oxford, UK, 1990.
4. Hassanzadeh, A.; Safari, M.; Hoang, D.H.; Khoshdast, H.; Albijanic, B.; Kowalczuk, P.B. Technological assessments on recent developments in fine and coarse particle flotation systems. *Miner. Eng.* **2022**, *180*, 107509. [CrossRef]
5. Vinnett, L.; Yianatos, J.; Alvarez, M. Gas dispersion measurements in mechanical flotation cells: Industrial experience in Chilean concentrators. *Miner. Eng.* **2014**, *57*, 12–15. [CrossRef]

6. Grau, R.; Heiskanen, K. Visual technique for measuring bubble size in flotation machines. *Miner. Eng.* **2002**, *15*, 507–513. [CrossRef]
7. Zhu, H.; Valdivieso, A.L.; Zhu, J.; Song, S.; Min, F.; Arroyo, M.A.C. A study of bubble size evolution in Jameson flotation cell. *Chem. Eng. Res. Des.* **2018**, *137*, 461–466. [CrossRef]
8. Zhu, H.; Valdivieso, A.L.; Zhu, J.; Min, F.; Song, S.; Arroyo, M.A.C. Air Dispersion and Bubble Characteristics in a Downflow Flotation Column. *Miner. Processing Extr. Met. Rev.* **2019**, *40*, 224–229. [CrossRef]
9. Randall, E.W.; Goodall, C.M.; Fairlamb, P.M.; Dold, P.L.; O'Connor, C.T. A method for measuring the sizes of bubbles in two- and three-phase systems. *J. Phys. E Sci. Instrum.* **1989**, *22*, 827–833. [CrossRef]
10. Grau, R.; Heiskanen, K. Bubble size distribution in laboratory scale flotation cells. *Miner. Eng.* **2005**, *18*, 1164–1172. [CrossRef]
11. Gomez, C.; Finch, J. Gas dispersion measurements in flotation machines. *CIM Bull.* **2002**, *95*, 73–78.
12. Tucker, J.; Deglon, D.; Franzidis, J.-P.; Harris, M.; O'Connor, C. An evaluation of a direct method of bubble size distribution measurement in a laboratory batch flotation cell. *Miner. Eng.* **1994**, *7*, 667–680. [CrossRef]
13. Khoshdast, H.; Hassanzadeh, A.; Kowalczuk, P.B.; Farrokhpay, S. Characterization Techniques of Flotation Frothers—A Review. *Miner. Processing Extr. Met. Rev.* **2022**, 1–25. [CrossRef]
14. Vinnett, L.; Yianatos, J.; Arismendi, L.; Waters, K. Assessment of two automated image processing methods to estimate bubble size in industrial flotation machines. *Miner. Eng.* **2020**, *159*, 106636. [CrossRef]
15. Mesa, D.; Quintanilla, P.; Reyes, F. Bubble Analyser—An open-source software for bubble size measurement using image analysis. *Miner. Eng.* **2022**, *180*, 107497. [CrossRef]
16. Schwarz, M.; Koh, P.; Wu, J.; Nguyen, B.; Zhu, Y. Modelling and measurement of multi-phase hydrodynamics in the Outotec flotation cell. *Miner. Eng.* **2019**, *144*, 106033. [CrossRef]
17. Bailey, M.; Gomez, C.; Finch, J. Development and application of an image analysis method for wide bubble size distributions. *Miner. Eng.* **2005**, *18*, 1214–1221. [CrossRef]
18. Grau, R.; Heiskanen, K. Gas dispersion measurements in a flotation cell. *Miner. Eng.* **2003**, *16*, 1081–1089. [CrossRef]
19. Sovechles, J.M.; Waters, K.E. Effect of ionic strength on bubble coalescence in inorganic salt and seawater solutions. *AIChE J.* **2015**, *61*, 2489–2496. [CrossRef]
20. Riquelme, A.; Desbiens, A.; Bouchard, J.; del Villar, R. Parameterization of Bubble Size Distribution in Flotation Columns. *IFAC Proc. Vol.* **2013**, *46*, 128–133. [CrossRef]
21. Karn, A.; Ellis, C.; Arndt, R.; Hong, J. An integrative image measurement technique for dense bubbly flows with a wide size distribution. *Chem. Eng. Sci.* **2015**, *122*, 240–249. [CrossRef]
22. Ma, Y.; Yan, G.; Scheuermann, A.; Bringemeier, D.; Kong, X.-Z.; Li, L. Size distribution measurement for densely binding bubbles via image analysis. *Exp. Fluids* **2014**, *55*, 1860. [CrossRef]
23. Vinnett, L.; Yianatos, J.; Alvarez-Silva, M. Gas dispersion measurements in industrial flotation equipment. In Proceedings of the 8th Copper International Conference, Copper 2013, Santiago, Chile, 1–4 December 2013.
24. Lau, Y.; Deen, N.; Kuipers, J. Development of an image measurement technique for size distribution in dense bubbly flows. *Chem. Eng. Sci.* **2013**, *94*, 20–29. [CrossRef]
25. Mazahernasab, R.; Ahmadi, R. Investigation of the Influence of Effective Parameters on Bubble Size Distribution in a Mechanical Flotation Cell by Image Analysis Method Modification. *Nashrieh Shimi Mohandesi Shimi Iran* **2016**, *31*, 133–146.
26. Iriarte, V. *Caracterización de la Dispersión de Gas en Celdas de Flotación Industrial*; Universidad Técnica Federico Santa María: Valparaíso, Chile, 2013.
27. Azgomi, F.; Gomez, C.; Finch, J. Correspondence of gas holdup and bubble size in presence of different frothers. *Int. J. Miner. Processing* **2007**, *83*, 1–11. [CrossRef]
28. Wang, J.; Forbes, G.; Forbes, E. Frother Characterization Using a Novel Bubble Size Measurement Technique. *Appl. Sci.* **2022**, *12*, 750. [CrossRef]
29. Hernandez-Aguilar, J.; Gomez, C.; Finch, J. A technique for the direct measurement of bubble size distributions in industrial flotation cells. In Proceedings of the 34th Annual Meeting of the Canadian Mineral Processors, Ottawa, ON, Canada, 22–24 January 2002; pp. 389–402.
30. Moreno, Y.S.; Bournival, G.; Ata, S. Classification of flotation frothers—A statistical approach. *Chem. Eng. Sci.* **2022**, *248*, 117252. [CrossRef]
31. Arends, M.A. *Reactivos de Flotación: Evaluación de Colectores y Espumantes*; Clariant: Muttenz, Switzerland, 2019.
32. Vinnett, L.; Alvarez-Silva, M. Indirect estimation of bubble size using visual techniques and superficial gas rate. *Miner. Eng.* **2015**, *81*, 5–9. [CrossRef]
33. Vinnett, L.; Sovechles, J.; Gomez, C.; Waters, K. An image analysis approach to determine average bubble sizes using one-dimensional Fourier analysis. *Miner. Eng.* **2018**, *126*, 160–166. [CrossRef]
34. Grau, R.A. *An Investigation of the Effect of Physical and Chemical Variables on Bubble Generation and Coalescence in Laboratory Scale Flotation Cells*; Helsinki University of Technology: Helsinki, Finland, 2006.